

Chemical Bonding State of Sulfur in Oxysulfide Glasses

Taro Asahi*, Yoshinari Miura**, Tokuro Nanba** and Hiroshi Yamashita***

*Department of Materials Engineering Nihama National college of
Technology 7-1 Yagumo-cyo Nihama-shi Ehime 792-8580, Japan

**Department of Environmental Chemistry and Materials, Faculty of
Environmental Science and Technology, Okayama University, 2-1-1,
Tsushima-naka, Okayama-shi 700-8535, Japan

***Department of Applied Chemistry, Faculty of Engineering, Ehime University, 3,
Bunkyo-cyo, Matsuyama-shi 790-8577, Japan

(Received September 23, 1998)

Simple binary $\text{Na}_2\text{S-SiO}_2$ oxysulfide glasses were prepared by a conventional melt-quench method in order to investigate the role of sulfur in glass structure and the electronic state. By X-ray photoelectron spectroscopy (XPS) measurement, S2p binding energy of the glass was observed at approximately 161eV which was close to that of ionic S^{2-} . The coordinating state around silicon atoms were investigated by ^{29}Si MAS-NMR measurement. The chemical shift observed from NMR supported that sulfur atom was joined to a silicon atom by substituting for an oxygen atom and was present as a non-bridging sulfide ion in low alkali content. On the other hand, it could be presumed that a portion of sulfur anions existed in an isolated state from the glass-network frame at high alkali content. The state of these sulfurs was also studied by Raman spectroscopy in detail.

Key words : Oxysulfide glass, S^{2-} , Non-bridging sulfur, XPS, ^{29}Si MAS-NMR, Raman spectroscopy

I. Introduction

Sulfur is widely used as colorant and refining agents in glass industry. Especially, it is well known that the sulfur compounds such as sodium sulfate act as refining agent in commercial glass batches. Recently these compounds are more effective than polyvalent metals such as As and Sb in terms of environmental chemistry. Sodium sulfate decompose in the melt and produce SO_2 gases. In this process, these formed bubbles grow larger for each combination and sweep the smaller bubbles containing O_2 and CO_2 in the melt. Consequently, sulfur compounds promote refining and homogenizing reaction as glass melting and a better quality of glass is produced at fast rate.¹ However, sulfur added to aid the refining of the glass may also be present as impurity and be incorporated in the resulting glass. Since the small amounts of sulfur remaining in glass products are closely related to coloration and affects their properties such as photo-absorption and chemical durability,² the removal of sulfurs after refining is great important to produce high quality products. On the other hand, the chemical state of sulfur in glass is essentially changed with glass composition, type of alkali, sulfur concentration, and the melting conditions. Behavior of sulfur in glasses, however, has not been made clear in the previous studies owing to uncertainty in correlation among these conditions and chemical state of sulfur. Therefore, it is also interesting to investigate the chemical state and the role of sulfur in

glass structure.

Sulfide ion is associated with glass network former in the same manner as oxide ion at the reducing atmosphere. Since sulfur has large ionic radius and small electronegativity, the glass containing sulfide ions has different electron density compared with oxide glass.^{3,4} Therefore, these glasses are expected to show electrical or optical character with peculiarities. In this study, due to the large solubility of sulfur alkali oxysulfide glasses were selected to investigate the role and effect of sulfur on the glass structure. Hanada et. al studied thermal and mechanical characteristics in oxysulfide glass system and compared them with the values in oxide glasses.^{5,6} Recently, the oxysulfide glasses are of interest in ionic conductive behavior.^{7,10} In the present study, glass network anions are partly substituted from oxide to sulfide ions in the system of sodium silicate glasses. Chemical bonding states of sulfur and coordinating state around silicon atoms were discussed.

II. Experimental Procedure

1. Preparation of glass samples

Binary glasses in the series $x\text{Na}_2\text{S-(100-x)SiO}_2$ were prepared from mixture of reagent grade silica sand and anhydrous sodium sulfide. The glass composition was selected at the range $x=25$ to 50 mol%(batch composition). The appropriate amounts of batch were dry-mixed completely. Melting was carried out in an alumina cru-

cible with a lid at 1400°C for 20 min under normal atmosphere. After melting, glasses were obtained by pouring melts onto a stainless steel plate. All the samples were preserved in a desiccator to avoid moisture attack.

Every obtained glass was reddish brown in color. The coloration changed to dark brown with increasing amount of sodium sulfide. Na₂S formed stable glass with SiO₂ at alkali concentration range less than 50 mol% in batch composition, but at larger alkali content than 50 mol%, the crystal deposition partly occurred. The transparent and homogeneous samples at glass forming range were used in various measurements.

2. XPS measurement

XPS spectra were measured with a Fisons Instruments "S-Probe ESCA (SSX100S)" equipped with monochromatic Al K α X-ray ($h\nu=1486.6$ eV). The rod shaped glass samples were broken under ultra high vacuum less than 1.33×10^{-7} Pa and the emitted photoelectrons from the fresh surface were analyzed. The control of surface charge-up was carried out by using both a low energy electron flux and an electrically grounded Ni mesh screen located about 1 mm above the sample surface. The photoelectron spectrometer was calibrated by using Au4f_{7/2} binding energy while the measured C1s binding energy for hydrocarbon impurities piling up on the sample surface in the vacuum for a few hours was calibrated as 284.6 eV.¹³

3. ²⁹Si MAS-NMR measurement

For the ²⁹Si MAS-NMR measurement, the sample glasses containing 0.01 mass% Fe₂O₃ for the total amount of batch were prepared. A JEOL JNM-CMX 300 spectrometer was employed to obtain the ²⁹Si MAS-NMR spectrum and operated at 59.74 MHz. The powdered glass samples were loaded into a zirconia spinner tube and spun at 4 kHz. The chemical shift of ²⁹Si was determined by using polydimethylsilan(PDMS) as a secondary standard. The chemical shift of PDMS was -34.11 ppm against tetramethylsilane (0 ppm). The pulse delay time between 4.5 μ s pulses (a $\pi/2$ pulse) was 5s.

4. Raman spectra

Raman spectra of the glasses were measured with a Nippon Bunko model JASCO NR-1000 Raman spectrophotometer using the 514.5 nm line of Ar⁺ laser as the exiting beam. The laser power was set at 60 mW and Raman spectra were measured at the rate of 120 cm⁻¹ per minute with the resolution of 0.5 cm⁻¹.

III. Results

1. XPS spectra

Fig. 1 shows the XPS wide scan spectrum of 40Na₂S 60SiO₂ glass. S2p signal is observed in this chart with Si 2p, O1s and Na1s signals. Since any signal of aluminum

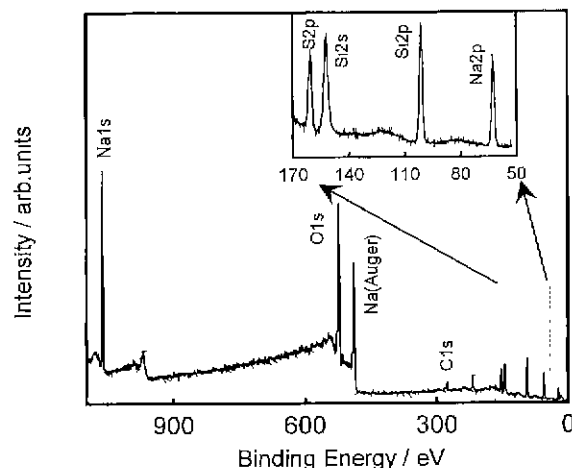


Fig. 1. XPS wide scan spectrum of 40Na₂S · 60SiO₂ glass (mol%) including narrow scan spectrum between 50 to 170 eV.

Table 1. Chemical Composition Calculated from XPS Spectra (Selected for Si2p, Na2s and S2p spectra) for Na₂S-SiO₂ glasses

Batch composition (mol%)		Analytical composition (mol%)		
Na ₂ S	SiO ₂	Na ₂ S	Na ₂ O	SiO ₂
30	70	11	21	68
35	65	14	23	64
40	60	21	20	59
45	55	24	22	54
50	50	24	26	50

orbits can not be seen, there is no contamination of the glass through chemical attack by aluminum ions from the crucible during melting. Table 1 shows analytical composition obtained from XPS spectra for Na₂S-SiO₂ glasses. Si2p, Na2p and S2p signals are selected for calculating chemical composition at the range between 50 to 170 eV due to the high intensity of each signal. With the peak intensity considering photoionization cross section, the amounts of oxygen are calculated from stoichiometric difference in amounts between cations and sulfurs in the glass. The ratio of SiO₂ to (Na₂S+Na₂O) estimated from analytical composition are almost equal to that of the batch composition. Therefore, it is found that the loss of alkali metal by volatilization was small and sulfurs in raw sodium sulfide were partly substituted for oxygen.

Fig. 2 shows S2p photoelectron spectrum for each sample. These peaks appear around at 161 eV. The 2p-orbit belongs in same azimuthal quantum number $l=1$. Therefore, S2p spectrum split into S2p_{1/2} and S2p_{3/2} peaks because of the spin-orbit interactions. Both S2p_{1/2} and S2p_{3/2} peak positions shift low energy about 0.3 eV for high alkali content samples at $x=40$ mol% or above. This fact indicates that the electron density of sulfur changes with glass composition. Furthermore, it is observed that shoulder-like peak is appeared at low binding energy region for the glasses at $x=45$ mol% or above. And the peak is gra-

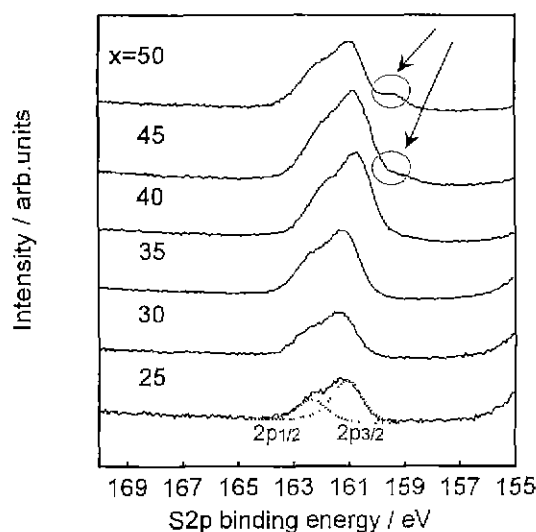


Fig. 2. S2p photoelectron spectra in the system of $x\text{Na}_2\text{S} \cdot (100-x)\text{SiO}_2$ ($x=25, 30, 35, 40, 45$ and 50) glasses. (The dotted curve are S2p_{1/2} and S2p_{3/2} spectra for $25\text{Na}_2\text{S} \cdot 75\text{SiO}_2$ glass)

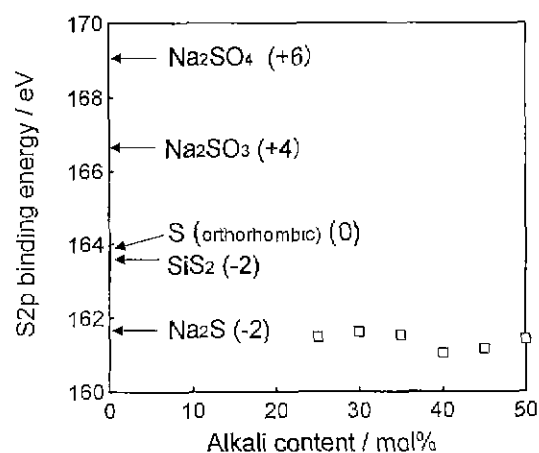


Fig. 3. S2p binding energy in the system of $x\text{Na}_2\text{S} \cdot (100-x)\text{SiO}_2$ (□) together with S2p of reference materials (arrow). (These values are the weight-mean of both S2p_{1/2} and S2p_{3/2} binding energies. The numbers inside bracket represent the valence number for sulfur)

dually clear. At the high alkali content, the change of glass structure was caused by the appearance of sulfurs having higher electron density. Fig. 3 shows the chemical shift of S2p binding energy for the glasses together with those of reference materials. These values are calculated by using the mean S2p binding energies weighted by S2p_{1/2} and S2p_{3/2} peak areas. The S2p mean values for the glasses are located near the value in Na_2S (161.7 eV). For high valence sulfurs, such as sulfur in Na_2SO_4 (S^{6+}) and Na_2SO_3 (S^{4+}), the electron densities are higher than that of crystalline sulfur (orthorhombic variety). From these results, neither sulfate ($:\text{SO}_4^{2-}$) nor sulfite ($:\text{SO}_3^{2-}$) anions can be seen in the glasses. Sulfurs in the glasses exist as sulfide (S^{2-}) having electron density equal to (-2) valence, and which show strong ionic bonding character.

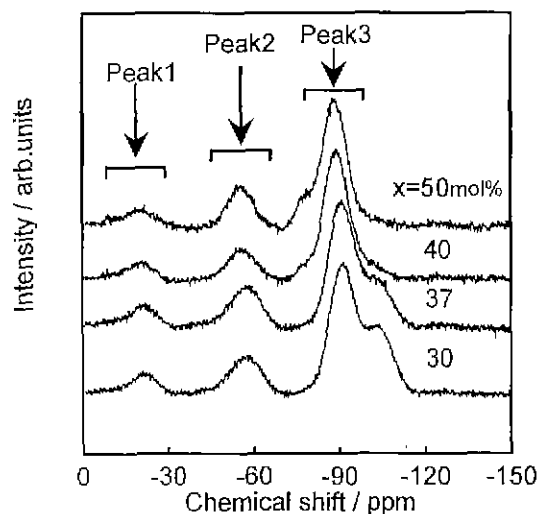


Fig. 4. ^{29}Si MAS-NMR spectra in the system of $x\text{Na}_2\text{S} \cdot (100-x)\text{SiO}_2$ glasses ($x=30, 37, 40$ and 50).

Table 2. The Fraction of Peak Area Calculated from ^{29}Si MAS-NMR Spectra for $\text{Na}_2\text{S}-\text{SiO}_2$ Glasses

Batch composition (mol%)		Peak area (%)		
Na_2O	SiO_2	Peak1	Peak2	Peak3
30	70	5.2	16.9	77.9
33	67	5.5	20.2	74.3
40	60	10.9	17.7	71.4
50	50	12.4	19.7	67.9

2. ^{29}Si MAS-NMR spectra

Fig. 4 shows ^{29}Si MAS-NMR spectra in the $\text{Na}_2\text{S}-\text{SiO}_2$ glass system. Three peaks appeared clearly in the range of 0 to -120 ppm. These peaks are regarded as "Peak1", "Peak2", and "Peak3" in turn from a high magnetic field side. Peak3 around -80 to -120 ppm are attributed to silicon atoms coordinated with four oxygen atoms. In full oxide glass systems, only Peak3 can be observed. However, both peak1 and peak2 appeared in the glass containing sulfur. Each spectrum can be fitted to several Gaussian peaks. The relative fraction of each peaks to the total peak area of [Peak1+Peak2+Peak3] are calculated from peak deconvolution. Table 2 shows the fraction of peak areas for each spectrum. The total peak area of [Peak1 and Peak2] increases with the amounts of sodium sulfide. Therefore, it is considered that Peak1 and Peak2 are attributed to silicon atoms coordinated sulfur atoms substituting for oxygen atoms. Hirai *et al.* concluded that the peaks between -25 and -55 ppm were attributed to silicon atoms coordinated sulfur and oxygen atoms simultaneously in the system of $\text{Li}_2\text{S}-\text{SiS}_2-\text{LiPO}_4$ glasses from ^{29}Si MAS-NMR measurement,¹⁵⁾ and our study also supported the formation of silicon atoms coordinated with both sulfur and oxygen atoms.

IV. Discussion

The O1s spectra in XPS for $\text{Na}_2\text{S}-\text{SiO}_2$ glasses split as

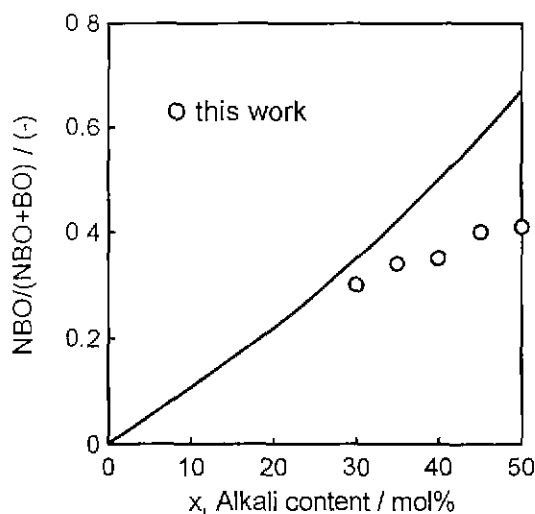


Fig. 5. The fraction of NBO to (BO+NBO) calculated from O1s XPS spectra in the system of $x\text{Na}_2\text{S} \cdot (100-x)\text{SiO}_2$ glasses. (The solid line is the values calculated for $x\text{Na}_2\text{O} \cdot (100-x)\text{SiO}_2$ glass)

with $\text{Na}_2\text{O-SiO}_2$ glasses and also make it clear that non-bridging oxygen(NBO) formed in sulfur containing glasses. The fraction of NBO to the total amount of oxygen in glasses calculated from peak area of O1s spectra are shown in Fig. 5 together with those of full oxide glasses. The solid line is the value which is calculated as an alkali metal ion forms a NBO in the full oxide glass. The fraction of NBO to total oxygen (=NBO+BO) decrease in the region of high alkali content compared with $\text{Na}_2\text{O-SiO}_2$ glasses, and it is suggested that the part of alkali metal ions are not role of NBO formation in $\text{Na}_2\text{S-SiO}_2$ glasses. Fig. 6 shows experimental ratio of non-bridging

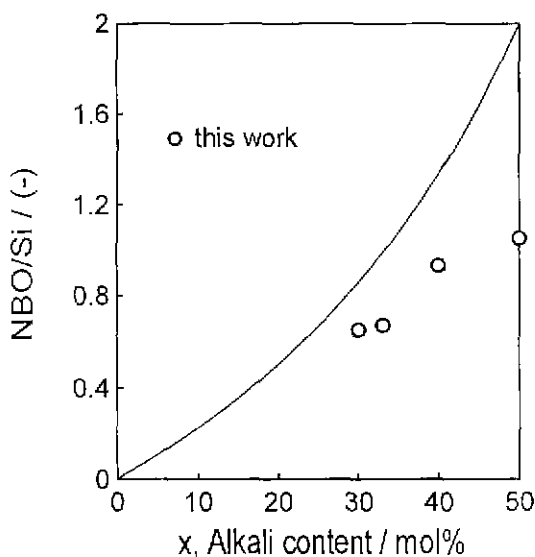


Fig. 6. The ratio of NBO coordinated to a Si atom calculated from ^{29}Si MAS-NMR spectra in the system of $x\text{Na}_2\text{S} \cdot (100-x)\text{SiO}_2$ glasses. (The solid line is the values calculated for $x\text{Na}_2\text{O} \cdot (100-x)\text{SiO}_2$ glass)

Table 3. S/Si Atomic Ratio Calculated from ^{29}Si MAS-NMR and XPS Spectra for $\text{Na}_2\text{S-SiO}_2$ Glasses

Batch composition	S/Si(-) (NMR)	S/Si(-) (XPS)
$30\text{Na}_2\text{S} \cdot 70\text{SiO}_2$	0.22	0.17
$40\text{Na}_2\text{S} \cdot 60\text{SiO}_2$	0.29	0.35
$50\text{Na}_2\text{S} \cdot 50\text{SiO}_2$	0.32	0.64

oxygen to a Si atom that are determined from Q_n distribution by using Peak3 in NMR measurement against glass composition, where n is the number of bridging oxygen atoms in a SiO_4 tetrahedral structure unit. The solid line in the figure is the same value which was calculated in Fig. 5. Since the values of NBO/Si for the sulfur containing glasses decrease in comparison with those of $\text{Na}_2\text{O-SiO}_2$ glasses, it is considered that the oxygen atoms around a silicon atom coordinated no sulfide ion are present as bridging oxygen(BO).

On the other hand, the silicon tetrahedron are coordinated sulfur atoms and sulfurs exist as S^{2-} having strong ionic bonding character. Therefore, sulfurs in the glasses are present as S^{2-} substituting NBO site rather than BO site in a SiO_4 tetrahedral structure unit. These S^{2-} terminate chemical bonding and correspond to non-bridging sulfur.

Furthermore, we calculated the atomic ratio of silicon to sulfur from S2p and Si2p XPS spectra to reveal the amount of sulfur coordinated to silicon atoms. For Fig. 4, Peak1 and Peak2 are not identified clearly how many silicon atom coordinates sulfur and oxygen atoms. However, we tried to estimate the ratio of silicon to sulfur on the assumption that both Peak1 and Peak2 are regarded as a silicon tetrahedron coordinating one sulfur and three oxygen atoms. Table 3 shows the comparison of the ratio of S2p/Si2p calculated from XPS with the ratio obtained from ^{29}Si MAS-NMR spectra. The amount of sulfur calculated from XPS sums up the overall sulfurs in the glass. On the other hand, ^{29}Si MAS-NMR spectra pick out the sulfurs coordinated to a silicon tetrahedron. Although the both values are approximately comparable in low alkali content, these values are quite different in high alkali content. This fact suggested the formation of the sulfur which are not bonded to silicon atom at high alkali regions. The shoulder peak appears at $x=45$ mol% or above in Fig. 2 also indicates the formation of sulfur isolated from glass network former.

In addition, it is expected that sulfur in the glasses is not only exist as S^{2-} but also as polysulfide species such as S_x^{2-} , S_x^+ and S_x .¹²⁻¹⁴⁾ In the system of $\text{Na}_2\text{S-SiO}_2$ glasses, the excess amount of sulfurs make glass structure loose and give rise to crystallization at last. Therefore, at high alkali content it is thought that the excess of sulfurs which isolated from the glass-network are more stable to be present as polysulfide clusters incorporated with the sodium ions rather than existed as non-bridging sulfur.

Raman spectra of the glasses were shown in Fig. 7. Ahmed et. al measured Raman spectra for sulfur-con-

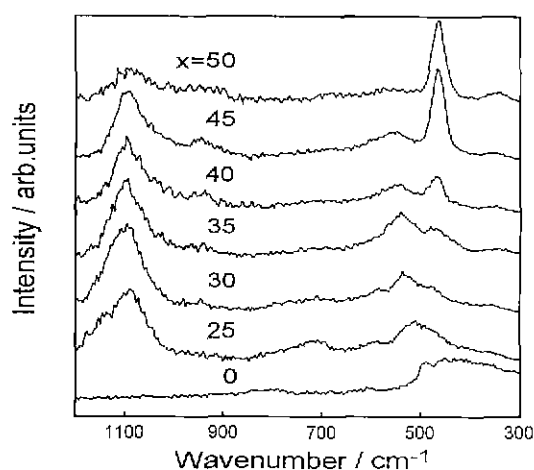


Fig. 7. Raman spectra of $x\text{Na}_2\text{S} \cdot (100-x)\text{SiO}_2$ glasses ($x=0, 25, 30, 35, 40, 45$ and 50).

taining alkali borate glasses, and they studied the origin of coloration for the glass in terms of the different state of sulfur.²⁴⁾ In their studies, the frequencies of the Raman bands associated with singly and doubly charged sulfur ions such as $\text{S}_x^{\cdot-}$ and S_x^{2-} ($x=2-6$) occur in the range 400 to 600 cm^{-1} . In this study, the intensity of peaks ranging from 400 to 500 cm^{-1} gradually increased with the amounts of sodium sulfide and the peak becomes sharper. It is also revealed that these peaks indicate the formation of polysulfide clusters coupled with excess sodium ions in the glasses.

V. Conclusion

Na_2S formed stable glass with SiO_2 by the conventional melt-quench method. The glass formation range in $\text{Na}_2\text{S}-\text{SiO}_2$ systems is similar to that of $\text{Na}_2\text{O}-\text{SiO}_2$ systems. The obtained glasses were reddish brown in color and it is confirmed that large amount of sulfurs were present in glass samples because of detecting $\text{S}2p$ spectrum by the XPS measurement. The value of $\text{S}2p$ binding energy was close to the value in Na_2S . Therefore, it was assumed that sulfurs in the glasses had an electron density close to ionic S^{2-} . Furthermore, by the ^{29}Si MAS-NMR measurement, three sharp peaks were detected between 0 and -120 ppm. The peaks between -25 and -55 ppm were attributed to a silicon tetrahedron coordinated both sulfur and oxygen atom simultaneously because these peaks could not be seen for full oxide glasses. The fraction of NBO estimated to XPS and ^{29}Si MAS-NMR spectra were decreased compared with that of $\text{Na}_2\text{O}-\text{SiO}_2$ glasses. From these results, it was considered that S^{2-} existed as non-bridging sulfur substituting oxide ion in SiO_4 tetrahedral units at the region of low alkali content. On the other hand, it was suggested that the formation of sulfur isolating from glass-network frame at the region of high alkali content. These sulfurs made clusters coupling with sodium ions, and Raman spectra showed these clusters as

the sharp peaks at the range between 400 and 500 cm^{-1} .

Acknowledgment

The authors would like to thank Mr.T.Ino in the graduate school of Okayama University for the XPS and Raman measurement.

References

1. P. M. DiBello, "Controlling the Oxidation State of a Glass as a Means of Optimising Sulphate Usage in Melting and Refining," *Glass Technology*, **30**, 160-165 (1989).
2. Haya Muller-Simon, "On the Interaction Between Oxygen, Iron and Sulfur in Industrial Glass Melts," *Glass Sci Technol*, **67**, 297-303 (1994).
3. B. Barrau, M. Ribes and M. Maurin, "Glass Formation, Structure and Ionic Conduction in the $\text{Na}_2\text{S}-\text{GeS}_2$ System," *J. Non-Cryst. Solids*, **37**, 1-14 (1980).
4. E. Robinel, B. Carette and M. Ribes, "Silver Sulfide Based Glasses (I)," *J. Non-Cryst. Solids*, **57**, 49-58 (1983).
5. T. Hanada, N. Soga and M. Kunugi, "Physical Properties of Germanate Glasses in $\text{Na}_2\text{O}-\text{GeO}_2$ and $\text{Na}_2\text{S}-\text{GeO}_2$ Systems," *J. Ceram. Soc. Japan*, **81**, 481-485(11) (1973).
6. T. Hanada, N. Soga and M. Kunugi, "Glass Formation and Structure of $\text{Na}_2\text{S}-\text{SiO}_2$ and $\text{Na}_2\text{S}-\text{B}_2\text{O}_3$ Glasses," *J. Non-Cryst. Solids*, **21**, 65-72 (1976).
7. H. Eckert, J. H. Kennedy, A. Pradel and M. Ribes, "Structural Transformation of Thiosilicate Glasses," *J. Non-Cryst. Solids*, **113**, 287-293 (1989).
8. H. Eckert, Z. Zhang and J. H. Kennedy, "Glass Formation in Non-oxide Chalcogenide Systems," *J. Non-Cryst. Solids*, **107**, 271-282 (1989).
9. T. Masahiro, K. Hirai, T. Minami, K. Takada and S. Kon-do, "Superionic Conduction in Rapidly Quenched $\text{Li}_2\text{S}-\text{SiS}_2-\text{Li}_3\text{PO}_4$ Glasses," *J. Ceram. Soc. Japan* **101**(11), 1315-1317 (1993).
10. K. Hirai, M. Tatsumisago, and T. Minami, "Thermal and Electrical Properties of Rapidly Quenched Glasses in the Systems $\text{Li}_2\text{S}-\text{SiS}_2-\text{Li}_x\text{MO}_y$," *Solid State Ionics*, **78**, 269-273 (1995).
11. S. Matsumoto, T. Namba, A. Osaka and Y. Miura, "Electronic Structure of Silicate Glasses by X-ray Photoelectron Spectroscopy," *Proc. 17th Inter. Cong. on Glass*, **3**, 72-77 (1995).
12. A. A. Ahmed, T. M. El-Shamy and N. A. Sharaf, "States of Sulfur in Alkali Borate Glasses," *J. Am. Ceramic. Soc.*, **63**(9-10), 537-542 (1970).
13. H. D. Schreiber, C. W. Schreiber and S. J. Kozak, "Novel Formulation of Amber Glass," *Am. Ceram. Soc. Bull.*, **71** (12), 1829-1835 (1992).
14. A. A. Ahmed, T. M. El-Shamy and N. A. Sharaf, "Raman Microprobe Investigation of Sulphur-doped Alkali Borate Glasses," *J. Non-Cryst. Solids*, **210**, 59-69 (1997).
15. K. Hirai, M. Tatsumisago, M. Takahashi, and T. Minami, " ^{29}Si and ^{31}P MAS-NMR Spectra of $\text{Li}_2\text{S}-\text{SiS}_2-\text{Li}_3\text{PO}_4$ Rapidly Quenched Glasses," *J. Am. Ceramic. Soc.*, **79**(2), 349-352 (1996).